



# COMBINED DIFFUSION PROCESS OF JOINING BIMETAL ELEMENTS OF HEAT EXCHANGE SYSTEM

Yu.A. KHOKHLOVA, V.E. FEDORCHUK and M.A. KHOKHLOV

E.O. Paton Electric Welding Institute, NASU, Kiev, Ukraine

A possibility of joining stainless steel to aluminium at lower temperatures owing to deposition on steel of a sprayed layer of commercial aluminium and molten gallium at different exposure times has been experimentally established. Optimization of microstructure and properties of a region of diffusion zone is achieved by application of a short-time heating with passing of low-voltage current.

**Keywords:** solid-phase welding, bimetal, aluminium, steel, gallium, adhesion, adhesion activator, reactive diffusion, reactive diffusion modeling, method of molecular dynamics, nanoindentation, diffusion coefficient

Special processes of joining dissimilar materials of the type of metal–nonmetal, metal–semiconductor and metal–metal in different combinations are often used in development and manufacturing of samples of sophisticated equipment. Here, in a number of cases the technology should provide a reliable joint at temperatures not exceeding 250 °C, as heating can lead to irreversible structural changes and lowering (loss) of service properties of materials as a whole. In addition, high requirements are made of the joints as to mechanical properties, vacuum tightness, electrical conductivity, etc.

The purpose of this work was finding a low-temperature process of joining stainless steel and aluminium alloy. Solution of this problem will allow producing bimetal assemblies for heat exchanger systems of aerospace microelectronics (Figure 1). The assembled item is 12Kh18N9T steel tube with outer diameter of 25 mm in a flange of AMg5 aluminium alloy of 100 mm length.

A promising technology for producing bimetal joints at up to 250 °C temperatures, in our opinion, is the diffusion process with gallium application [1]. Gallium melts at the temperature of about 30 °C, readily wets and dissolves most of the metals and solidifies with

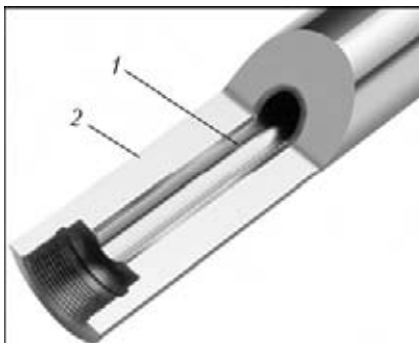


Figure 1. Bimetal block of heat exchange system: 1 – stainless steel; 2 – aluminium

volume increase that allows applying it as activator of adhesion of the surfaces being joined with subsequent volume diffusion. Activation consists of a mechanochemical process, including fragmentation, delamination and dissolution of oxide films, wetting of juvenile surfaces, as well as inter- and intragranular diffusion. Mechanochemical activation leads to increase of the solubility of difficult-to-dissolve materials, acceleration of chemical reactions, increase of catalytic and improvement of physico-technical properties, and lowering of material surface activation temperature in the solid-phase process of their joining [2].

In order to form a strong steel-aluminium joint and prevent its embrittlement, a layer of commercial aluminium AD1 was sprayed on the steel tube surface (Figure 2). The process of spraying is performed by microplasma method, i.e. heating, dispersion and transfer of condensed particles of spraying material with formation of 200 µm layer on the substrate. MPN-004 system was applied for spraying, which allows aluminium to be deposited at substrate temperature of up to 150 °C. Formation of metal coatings with fixing of hard metal particles, characterized by high kinetic energy, on the substrate surface, occurs at high-speed impact (Figure 2, b) that provides high adhesion properties.

The bimetal assembly materials have as close as possible values of the coefficient of linear temperature expansion, thus providing an equivalent joint without part distortion (Table 1). As to the coefficient of heat conductivity, the materials for the heat exchange system are selected so that the radiator from AMg5 alloy ensures heat removal from the steel core through an interlayer of intermediate metal (gallium).

Gallium layer of 0.05–0.15 mm thickness was applied on the surfaces being joined by the method of mechanical rubbing, parts were joined by the mated surfaces, and diffusion hardening of the gallium interlayer was performed at assembly heating in the vacuum furnace or by passing current up to 140 and 250 °C. An advantage of second heating is its short duration, and heat evolution chiefly in the zone of contact of surfaces being joined. As a result, reactive diffusion initiates faster, heat evolution into the ma-

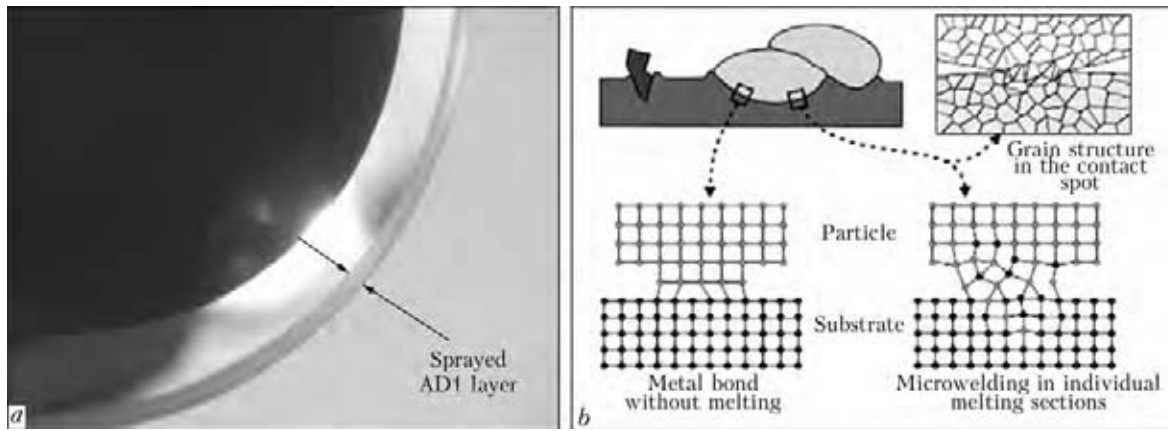


Figure 2. Fragment of stainless tube with sprayed layer of aluminium AD1 (a) and schematic of metal coating formation (b)

Table 1. Physical properties of joined materials

Material	Specific heat capacity, J/(kg·K), at 100 °C	Coefficient of linear thermal expansion·10 <sup>6</sup> , K <sup>-1</sup> , at 100 °C	Heat conductivity coefficient, W/(m·K)	Young's modulus, GPa	Melting temperature, °C
AMg5 aluminium alloy	922	24.7	126	71	625
AD1 commercial aluminium	945	24	226	71	660
12Kh18N9T stainless steel	469	17	16	189	1300
Commercial gallium	–	–	28.1	10–45	30.15

terial is reduced, and diffusion layer depth decreases, that is favourable for the joint microstructure and mechanical properties. A condition for formation of a sound joint is tight fitting of the parts and removal of gallium flash from the end faces. Gallium fillets filling the item end face gaps at solidification with volume increase, may lead to formation of extended cracks in the aluminium flange bulk. Temperature was controlled during heating with a thermocouple and thermal imager Fluke Ti25.

Analysis of the structure and distribution of chemical elements showed that gallium diffusion occurs in the direction of AMg5 alloy, whereas no chemical presence of gallium was found in steel (Figure 3). A multistage process of formation of metastable phases from the main alloying elements of AMg5 alloy and gallium proceeds with formation of a hard intermetallic layer and increase of its melting temperature [3]. Analysis of binary diagrams of equilibrium state showed that the temperature of transition into the

liquid state of intermetallics of Ga–Mg and Ga–Zn systems is equal to more than 285 °C, and from 254 up to 1000 °C for Cu–Ga system.

Liquid gallium diffused along the aluminium grains (Figure 4) to the depth of up to 3 mm. This resulted in formation of a layer of solid solution and intermetallic phases in the gap and adjacent aluminium volume. Transmission electron microscopy examination of the fine structure of AD1/AMg5 joint zone through a gallium interlayer revealed the following. AD1 structure is characterized by a comparatively equilibrium state that is indicated by formation of an equiaxed substructure uniformly distributed through the entire volume of metal, adjacent to the joint plane, as well as formation of perfect (contracted) boundaries and subboundaries (Figure 5, a).

Structure in the joint zone (from AMg5 side) is characterized by appearance of structural-phase formations (interlayers), having a clear orientation along the line of gallium deposition with about 0.81–

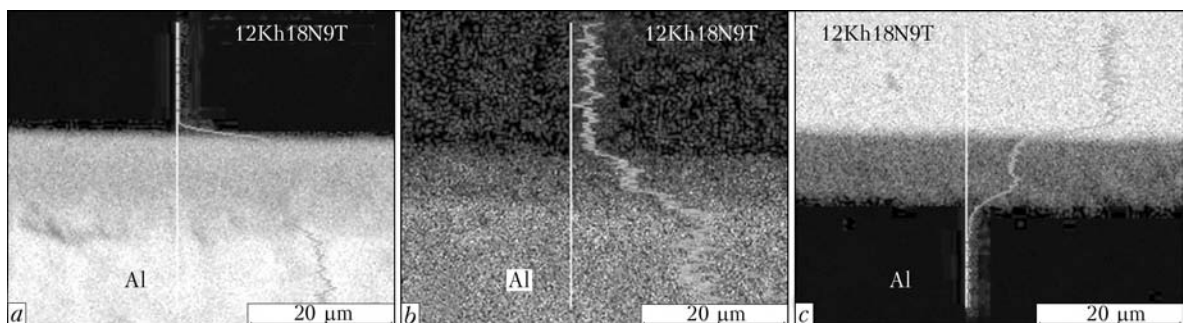
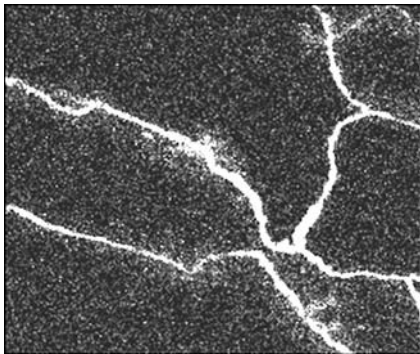


Figure 3. Maps of distribution of aluminium (a), gallium (b) and iron (c) across the section of stainless steel and aluminium joints (SEM)



**Figure 4.** Maps of gallium distribution in the volume of AMg5 alloy as a result of reactive diffusion ( $\times 1000$ ) (SEM)

1.10  $\mu\text{m}$  interlayer thickness, and different phase compositions. A certain part of the interlayers consists of practically clean gallium. Gallium sections of the interlayers have an either columnar substructure with growth direction normal to the line of gallium deposition (Figure 5, *b*), or a comparatively equiaxed structure of Ga-phases (Figure 5, *c*) with intergranular precipitates of  $\text{Ga}_2\text{Mg}$ -phases. The gallium-containing regions of such interlayers are characterized by an equilibrium structural state.

It should be noted that phase composition of the interlayers becomes more complicated at shifting from the line of gallium deposition towards AMg5. At removal for up to 300  $\mu\text{m}$  distance from the joint plane, formation of the structural-phase state is observed, which is characterized by an increase of volume fraction of dispersed phase precipitates ( $h \times l \sim 0.03 \times 0.06 \mu\text{m}$ ;  $0.06 \times 0.1 \mu\text{m}$ ;  $0.03 \times 0.37 \mu\text{m}$ ;  $d \sim 0.03\text{--}0.10 \mu\text{m}$ ) of  $\text{Ga}_2\text{Mg}$ ,  $\text{Ga}_2\text{Zn}$ ,  $\text{Al}_6\text{CuMg}_4$ ,  $\text{Al}_2\text{CuMg}$ ,  $\text{Cu}_9\text{Ga}_4$  composition. Here, in addition to densely and uniformly distributed dispersed phases of various stoichiometric composition, also phase formations of a special type are observed in the diffusion zone: these are more massive ( $h \times l \sim 0.65 \times 1.70 \mu\text{m}$ ;  $0.73 \times$

$\times 1.07 \mu\text{m}$ ;  $0.75 \times 2.35 \mu\text{m}$ ) extended «strip-type» phases of a complex composition, forming in the direction parallel to the fusion line (Figure 5, *d*).

Structure of this type of phase formations is quite clearly visible on TEM images, and its composition corresponds to  $\text{Ga}_2\text{Mg}$  with dispersed  $\text{Ga}_2\text{Zn}$ ;  $\text{Cu}_9\text{Ga}_4$  of sizes  $d \sim 0.017\text{--}0.030 \mu\text{m}$ . In addition, it is particularly characteristic that «strip-type» phase precipitates are surrounded by fringes around their contour, consisting of dense clusters of highly dispersed phases of various composition:  $\text{Ga}_2\text{Mg}$ ;  $\text{Ga}_2\text{Zn}$ ;  $\text{Cu}_9\text{Ga}_4$ , etc. Thus, it can be stated that the diffusion layer growth occurs with volume increase due to rotation of AMg5 grains at growth of newly-formed phases.

Such a graded distribution of phases, their definite clear orientation further promote non-uniformity of dislocation density distribution, and, therefore, formation of stress raisers in the respective zones of the studied joint. At nanoindentation testing [4, 5] of the influence of gallium reactive diffusion on the properties of AMg5 alloy, an anomalous adsorption lowering of strength and metal softening (Rebinder effect) were found [6]. Figure 6 shows the difference in dimensions of Berkovich indenter imprints in the central and grain-boundary region of the structure of AMg5 alloy sample at heating up to 250  $^\circ\text{C}$  in the vacuum furnace for 1 h.

Stabilization of aluminium mechanical properties occurs at final solidification of solid-liquid phases with gallium. Solidification duration corresponds to the time of new phases growing for the thickness of deposited gallium interlayer [7]. Determination of the moment of microstructure stabilization at minimum width of the diffusion zone and achievement of satisfactory mechanical properties, depending on heating time, were simulated experimentally and by molecular dynamics method at temperatures of 50, 140 and

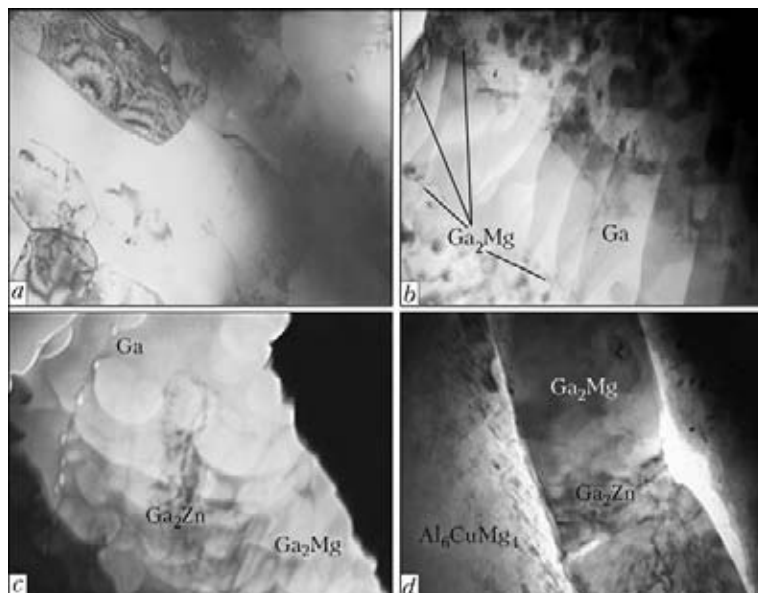


**Figure 5.** AD1 microstructure (*a* –  $\times 15,000$ ), laminated rounded and columnar fragments of gallium (*b*, *c*) and phases (*d*) in the intergranular space of AMg5 alloy ( $\times 50,000$ ) (TEM)



**Table 2.** Dependence of diffusion layer width on exposure time and diffusion coefficient at heating up to 140 °C

Temperature, °C	Diffusion layer width, cm	Time during which diffusion advanced to specified depth, s	Diffusion coefficient · 10 <sup>-7</sup> , cm <sup>2</sup> /s
50 (furnace)	0.13	36000	2.35
140 (same)	0.15	36000	3.13
140 (same)	0.30	86400	5.20
140 (current)	0.01	60	4.76
140 (same)	0.02	120	33.30
250 (same)	0.05	210	104

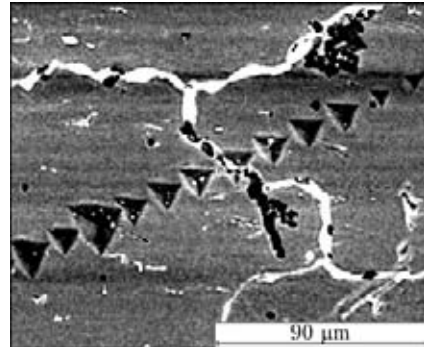


**Figure 6.** Microstructure of AMg5 alloy with indenter imprints (SEM)

250 °C. It is known that the mechanism of gallium diffusion in aluminium is mainly related to the ratio of atomic radii: closeness of dimensions of gallium and aluminium atoms promotes gallium diffusion through aluminium vacancies. Therefore, modelling of the dynamics of aluminium atomic lattice change was conducted by the vacancy mechanism. A limited quantity of atoms was considered in the model (5325), which was, however, sufficient for the experiment to have

physical sense. 3D models of the crystalline lattice were assigned according to aluminium lattice period. Modelling results are atom coordinates in each step. Difference of coordinates was used to determine atom displacement. Of all atom displacements those without jumping (atom oscillation around the node) are not taken into account. Displacements, leading to jumps, were used to calculate the diffusion coefficient. Activation energy was determined by Arrhenius graph in  $\ln D(1/T)$  coordinates by tangent of angle.

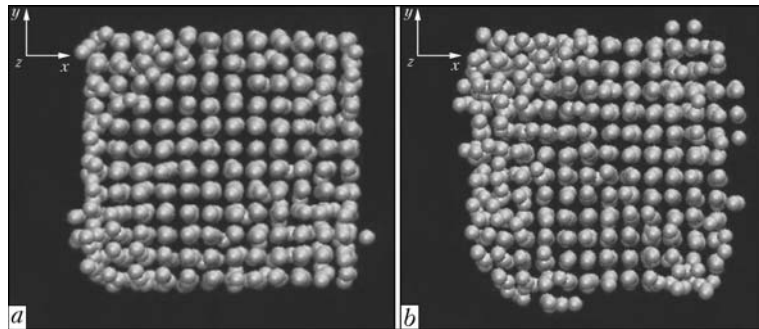


**Figure 7.** Dynamics of variation of aluminium crystalline lattice with temperature rise (volume modelling by molecular dynamics method): a – T = 140; b – 250 °C

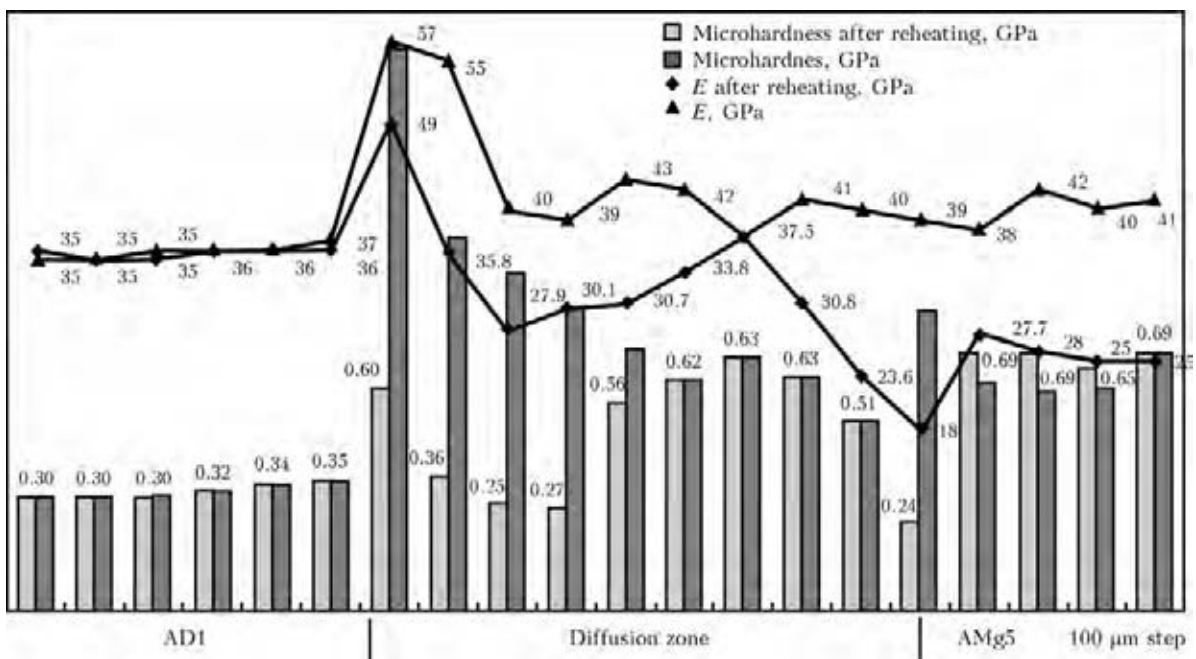


**Figure 8.** Diagram of Meyer hardness distribution and Young's modulus E in diffusion joint on the boundary of AD1 with AMg5 at heating by current up to 140 °C and after reheating up to 280 °C

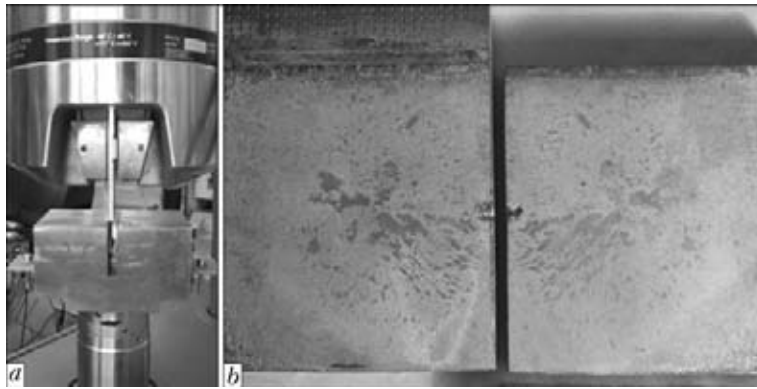


**Figure 9.** Shear strength tests in tensile testing servohydraulic machine MTS (a) of flat overlap sample of AMg5-Ga-AD1 diffusion joint (a) and sample fractograph after testing (b)

Increase of the number of atom jumps, contributing to diffusion, is due to greater activity of atoms with temperature rise [8] (Figure 7, a) and rises from 28 (at 50 °C) up to 4346 (at 250 °C). Diffusion coefficients are equal to,  $m^2/s$ :  $2.86 \cdot 10^{-10}$  for 50 °C,  $7.56 \cdot 10^{-10}$  for 140 °C and  $4.74 \cdot 10^{-9}$  for 250 °C. Activation energy is equal to 0.62 eV.

Experimental modelling of the dependence of diffusion layer growth on temperature-time exposure of AD1-Ga-AMg5 samples confirmed the general tendency (Table 2): with increase of temperature and time of heat treatment gallium rheological properties are enhanced and an extended diffusion zone forms.

Furtheron, repeated heat treatment of all the samples in the furnace up to 280 °C for 10 h was conducted to determine process optimum temperature and time, at which the diffusion layer structure will preserve its properties. It is established that in samples processed at temperature of 140 °C by passing current no significant change of either diffusion layer microstructure, or its mechanical properties is observed (Figure 8).

At shear strength testing (Figure 9, a) to GOST 6996-66 (material thickness  $a = 6$  mm, gauge length  $l = 125$  mm, grip  $h = 60$  mm, overlap  $b = 40$  mm) breaking load  $F$  was equal to 4710 N, shear stress was 2.94 MPa, respectively, that is much higher than the minimum value required by the specification (0.2 MPa). One can see in the fractograph of fracture plane (Figure 9, b) that at joint assembly complete wetting and adhesion of the surfaces being joined occurred with minimum edge effect. According to the specification the summary area of joint defects is less than 10 %.

Maximum breaking force  $G$  of «anti-shear» at diffusion overlap area of  $15 \times 15$  mm<sup>2</sup> was equal to 400 N. Tearing force (maximum breaking force per a unit of overlap surface) was  $\tau \approx 1.7$  MPa.

Shear strength of circular samples was equal to 9–11 MPa.

It should be noted that application of polymer-based metal adhesives mixed with metal powders for assembly of heat exchange systems of microelectronics insulation is not rational, as the heat conductivity coefficient in such materials is many times lower than in metals (0.02–0.6 W/(m·K)).

**Shear fracture force of aluminium alloy joints, MPa**

Al-Al (adhesive joint, liquid metal	
Fe1 WURH [9]) .....	2.4
Al-Al (adhesive joint), polymer adhesive	
ABRO [10] .....	5.9
AMg5-AD1 (required by specification) .....	0.2
AMg5-Ga-AD1 (welding by passing current at 140 °C) .....	2.94

Retrofitting of the technology of solid-phase joining of steel-aluminium assembly through an interlayer of eutectic gallium resulted in various variants of assembly of heat exchange system component (Figure 10) with a high value of shear fracture force.

In conclusion it should be noted that a possibility of joining stainless steel to aluminium at 140 °C temperature using a sprayed layer of commercial aluminium and gallium interlayer was established experimentally. The most favourable microstructure and properties of the diffusion zone are observed at application of heating by low-voltage passing current. Strong permanent joints of bulk configuration were produced without surface melting or distortion of

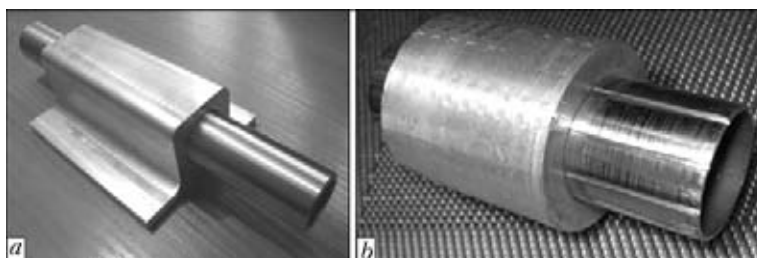


**Figure 10.** Model samples of steel-aluminium diffusion joint made at 140 °C temperature over a conical surface (a) and with longitudinal slots (b)



parts. This process of joining the bimetal assembly is recommended for joining over closed, mated or cylindrical surfaces, using the effect of thermal shrinkage and reduction.

1. Ishchenko, A.Ya., Khokhlova, Yu.A., Fedorchuk, V.E. et al. (2010) *Technological features of producing joints of commercial aluminium with AMg5 alloy at activation of surfaces being joined by molten gallium*. Transact. Nikolaev: NUK, 68–74.
2. Avvakumov, E.G. (2009) *Fundamentals of mechanical activation, mechanosynthesis and mechanochemical technologies*: Integration projects. Novosibirsk: Nauka.
3. Khokhlova, Yu.A., Fedorchuk, V.E., Khokhlov M.A. (2011) Peculiarities of intergranular mass transfer of gallium in aluminium alloy during solid phase activation of surfaces being joined. *The Paton Welding J.*, **3**, 13–15.
4. Ishchenko, A.Ya., Khokhlova, Yu.A. (2009) Evaluation of mechanical properties of microstructural constituents of welded joints. *Ibid.*, **1**, 34–37.
5. Khokhlova, Yu.A., Khokhlov, M.A. (2009) Nanoscale effect in diffusion joints with gallium. In: *Abstr. of Int. Conf. on Welding and Related Processes*. Nikolaev: NUK, 111.
6. Likhman, V.I., Shchukin, E.D., Rebinder, P.A. (1962) Physiko-chemical mechanics of metals. In: *Adsorption phenomena in processes of deformation and fracture of metal*. Moscow: AN SSSR.
7. Tikhomirova, O.I., Pikunov, M.V. (1969) Influence of shape and size of second component particles on properties of gallium solders. *Poroshk. Metallurgiya*, **82(12)**, 51–56.
8. Poletaev, G.M., Starostenkov, M.D. (2010) Contributions of different mechanisms of self-diffusion to fcc metals in equilibrium conditions. *Fizika Tc. Tela*, **52**, Issue 6, 1075–1082.
9. [www.svarka-lib.com/node/298/print/64.html](http://www.svarka-lib.com/node/298/print/64.html)
10. [www.autodela.ru/main/top/test/svar](http://www.autodela.ru/main/top/test/svar)

## INFLUENCE OF VIBRATION OF PARTS ON STRUCTURE AND PROPERTIES OF METAL IN SURFACING

Ch.V. PULKA<sup>1</sup>, O.N. SHABLY<sup>1</sup>, V.S. SENCHISHIN<sup>1</sup>, M.V. SHARYK<sup>1</sup> and G.N. GORDAN<sup>2</sup>

<sup>1</sup>Ternopol Ivan Pulyuj National Technical University, Ternopol, Ukraine

<sup>2</sup>E.O. Paton Electric Welding Institute, NASU, Kiev, Ukraine

Presented are the investigation results of structure and properties of metal deposited by induction method with superposition of vibrations in a period of melting of a surfacing consumable. It is shown that the superposition of vibrations leads to improvement of wear resistance of the deposited metal due to refinement of its structure.

**Keywords:** induction surfacing, inductor, specific power, vertical and horizontal vibrations, deposited metal, structure, wear resistance

An induction surfacing using powders from high-carbon chromium alloy PG-S1 (sormite 1) is widely used for manufacture of operating elements of agricultural machines: plough shares, blades of top cutters, chisels of cultivators etc. At that a deposited metal has a coarse-grain structure with inclusions of coarse chromium carbide [1, 2].

A new technology of induction surfacing using vibrations [3–6] was proposed for refinement of structure and improvement of properties of the deposited metal. It lies in the fact that a part is subjected to vertical and horizontal vibration at the moment when a powder charge is in a molten state. At that, direction of oscillation application (Figure 1) as well as their frequency and amplitude have a great importance.

Investigations of structure, microhardness of structural constituents and wear resistance of the metal deposited by induction method with and without vibration superposition were performed for evaluation of the efficiency of developed technology. The flat samples from steel St3, i.e. sample 1 without vibration, 2 and 3 with vertical and horizontal vibrations, correspondingly, were deposited for performance of the investigations by induction method using a charge containing PG-S1 alloy powder. Surfacing was carried out on a high-frequency generator of VChG 6-60/0.44

type at constant specific power  $W$  and time of deposition  $t$  (Figure 1, *b*). The modes were similar for all three variant of surfacing, i.e. circuit voltage 5.4 kV; anode voltage 10 kV; circuit current of lamp 1.2 A; anode current of lamp 2 A; deposition time 35 s; oscillation amplitude 0.2 mm at 50 Hz frequency.

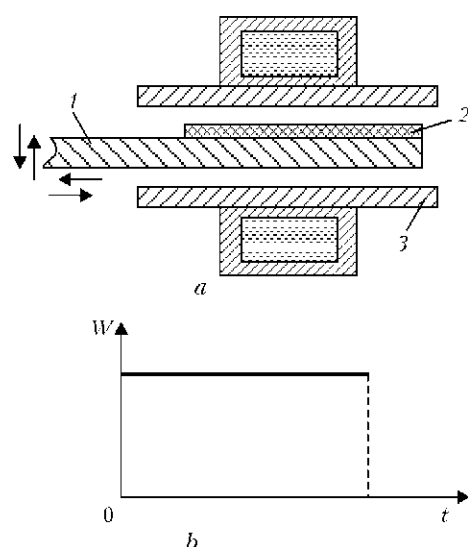


**Figure 1.** Surfacing scheme (*a*: 1 – part being deposited; 2 – powder-like charge; 3 – inductor; arrows show direction of vibration application – vertical or horizontal), and specific power  $W$  of generator in the process of surfacing (*b*)